Contents

Chapter 1

Spectral Analysis

A fundamental aspect of the Plasma Coagulation Controller is what species are produced and deposited during its application. Various studies observed the spectrum of plasma DBD discharge in air at atmosferic pressure and ambient temperature ([4], [5]), meanly it presents peaks relative to reactive species from water, oxygen, nitrogen and its oxides at visible wavelenght, from 200 to 880 nm.

We are intersted in plasma that contains molecules involved in blood coagulation mechanisms, Reactive Oxidant Species (such as hydroxil radical OH) and Reactive Nitrogen Species (derived from nitric oxide NO) ([11]). In this spectroscopy study is given particular attention to them and their precursor, i.e. the presence of transitions relative to hydroxil, oxygen and molecular nitrogen.

1.1 Radiation emission

As remembered in previous chapters, at the exit of source head is produced plasma from a mixture gas of helium or argon and air, so there is a certain fraction of free charges inside the plume fo plasma. Along free electrons, there are ions and species that colliding with them are in an excited state, metastable or with small lifetime. All those reactive species partecipe in different reactions, and also in excitation and de-excitation reactions with conseguent emission of radiation. When an electron goes from state p at higher energy to state k of lower energy, is emitted radiation with central wavelenght λ_0. Power emitted by this radiation is given by radiant flux $d\phi_\lambda$ and selecting a solid angle as in figure, is possible to define radiance L_λ, and intensity I, as in equations 1.1. Intensity for a radiation ultimately depends on $n(p)$, population density for state p, and Einstein Coefficient for the transition A_{pk} that is typical for the transition ([1]).

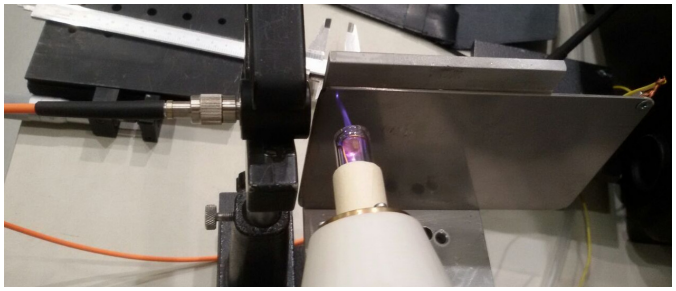

Figure 1.1: Setup of the experiment: there is the working source, the metal target and the optical setup on the left.

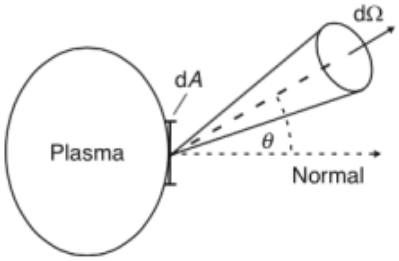

$$\lambda_0 = \frac{hc}{E_p - E_k}$$
$$L_\lambda = \frac{d^2\phi_\lambda}{dA\cos(\theta)d\Omega} \tag{1.1}$$
$$I = \int L_\lambda d\lambda = n(p)A_{pk}$$

Using air as gas, composed by molecules, at visible wavelenght are observed vibronic transitions where molecule goes from a vibrational state to another, with a change of vibrational quantum number ν, and/or from a rotational state to another, with change of quantum number J ([6], [13]). When there is a vibrational transition, each line corresponds to different numbers $\nu' - \nu''$, these are transitions well spaced in the spectrum, easy to recognize. Rotational transitions gives birth to bands of little-spaced peaks hard to resolve whitout an efficient spectrometer.

There are many reactions involving oxygen and nitrogen (see for example [9]), in this study we determine only principal transition observable with our spectrometer, to know dominant reactive species present in our plasma plume.

1.2 Experimental setup

For the source it's used a prototype that presents electrical specifics and settings same as source A described in previous chapters. A metal plate is positioned as target at a distance of 10 mm from plasma exit. To ignite plasma is used helium, with flow set to 2 L/min. To measure emission it's used a spectrometer IsoPlane, that thanks to diffraction separates emissions with different wavelenghts using a plane grating. The spectrometer has a focal lenght of 320 mm and is equipped with three different gratings: 150, 1200 and 2400 gg/mm, corresponding to different resolutions of 0.26, 0.03 and 0.01 nm. As in figure 1.1, light emitted by plasma is collected with a quartz lens and passes trough an optical fiber connected to the spectrometer entry, while at the spectrometer exit there is a CCD camera of 2048 pixels and a count limit of 65 000.

Once a grating is chosen, the acquisition system can be set at a starting wavelenght and from there it takes measures until the end of the CCD, so for a wavelenght interval different for different gratings. For every measure is selected an appropriate acquisition time that permits to observe peaks with a good count number and avoid saturation.

It's important to stress out that, with this measuring method and due to complexity of plasma reactions and composition, it's not possible to extrapolate quantitative considerations between different species concentration. However it's possible to recognize the presence of certain species and make some considerations watching spectra variation with different experimental setup.

An intersting parameter is the working distance between source's head and target, so we observe spectra focalizing the lens in two different positions:

- position 1: as close as possible to plasma exit point
- position 2: close to the target, at 10 mm from plasma exit point

Reactions that produce and recombine reactive species, and consequently density and lifetime of species, are influenced by electric field and duration of the discharge. We observe spectra changing amplitude and frequency of the pulse, with tree different combinations that corresponds to different power coupled with the discharge:

- low: $f = 5\,\text{kHz}$ and $\Delta t = 15\,\mu\text{s}$
- medium: $f = 10\,\text{kHz}$ and $\Delta t = 10\,\mu\text{s}$
- high : $f = 15\,\text{kHz}$ and $\Delta t = 10\,\mu\text{s}$

1.3 Line recognition

To see what's generally produced in a discharge is taken a spectrum for the entire wavelenght's region intersted, from 230 to 800 nm, with standard setup of medium power and position 1. First is made a rapid acquisition with the lowest resolution possible, to see intersting regions and have an idea of required exposition times. After that is made a slow acquisition with higher resolution for all wavelenghts. The entire spectrum is reconstructed attaching different spectra, showed in figure 1.2, where are labelled principal transitions. For every measure is taken also a background spectrum, without plasma, to recognize peaks that are not from the plasma.

Data is read with IDL routines ([]) and analyzed with ROOT TSpectrum.h library ([]). Every spectrum is divided by its exposition time, to normalize different measures. Then is estimated the white noise contribution as mean value from a portion of the spectrum that doesn't presents peaks and its subtracted to the counts for each wavelenght. Peaks are then found with TSpectrum functions (where is possible to set a treshold in heigth and the general width for lines to be searched) and peaks from background are isolated in plasma spectra. Definitive position for each transition is found with a gaussian fit in an interval that takes into consideration the asymmetry where it's needed.

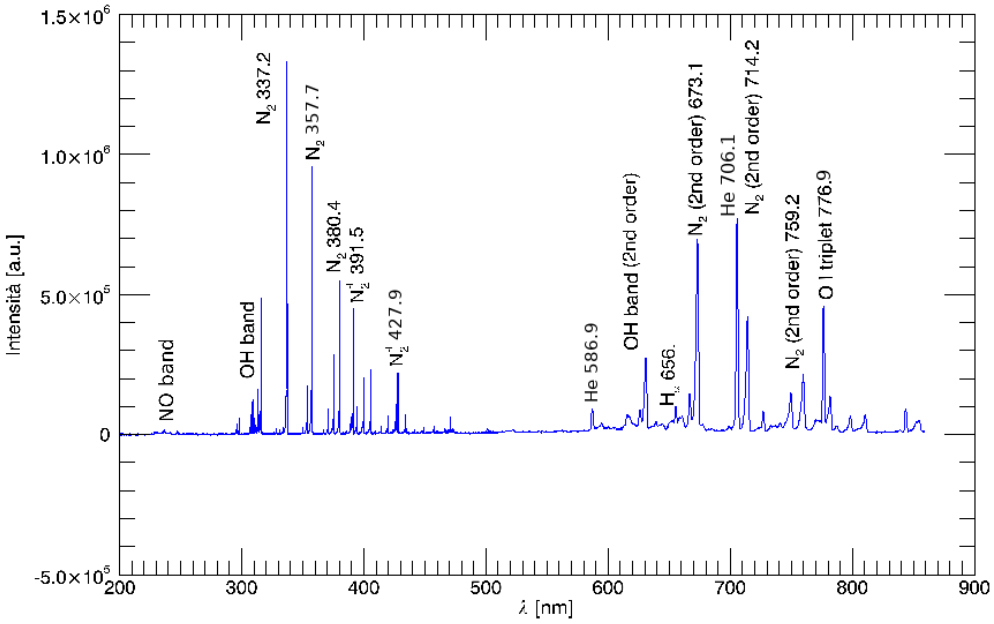

Figure 1.2: Spectrum with an helium flow of 2 L/min, pulse parameters of $f = 5\,\text{kHz}$ and $\Delta t = 16\,\mu\text{s}$, optical position 1, near plasma exit

As said before, this study is focused on measure related to ROS and NRS, so in lines for NO, OH and N_2.

NO lines Are observed two doublets for the transition $A^2\Sigma^+ - X^2\Pi$ with vibrational numbers (0-0) and (0-1) ([8], [12]), presented in table 1.1. Intensities for the peaks are normalized with maximum value of 1000 for the acquisition, the table shows as the intensities for this transition is very low. Other transition relative to this molecule have even lower relative intensity and are not observed in our study.

λ [nm]	I [arb.u.]
236.31 ± 0.24	27
237.00 ± 0.15	26
247.02 ± 0.05	28
247.86 ± 0.12	27

Table 1.1: Peaks measured for NO.

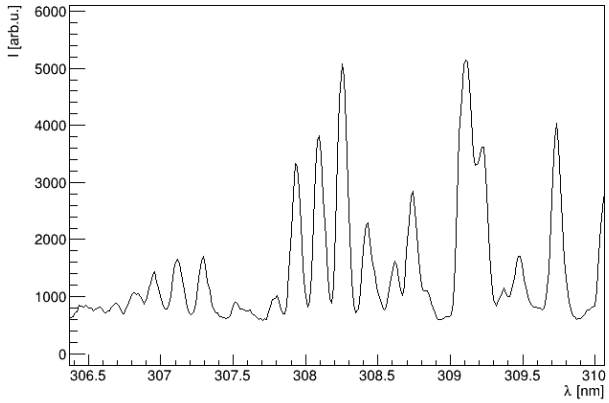

Figure 1.3: Zoom for OH peaks

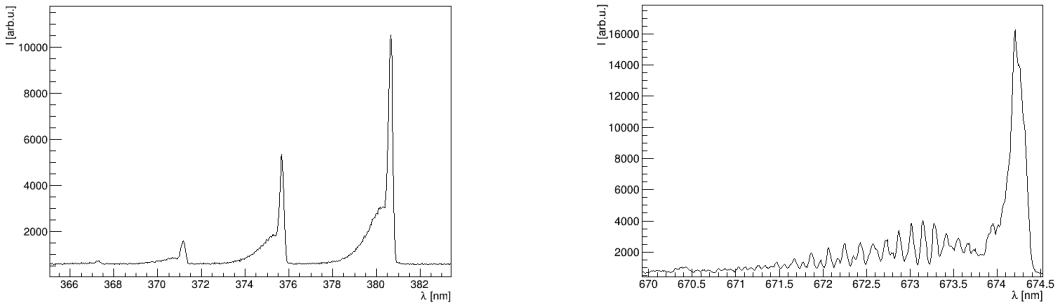

(a) Transitions with $\Delta\nu = 2$ **(b)** Strongest line (0-0)

Figure 1.4: Zoom for N_2 transitions.

OH lines Is observed the rotational band for transition ($A^2\Sigma$, $\nu' = 0 \rightarrow X^2\Pi$, $\nu'' = 0$), observing 13 principal lines ([7]). In figure 1.3 a zoom on the spectrum, in table 1.2 peak values.

N_2 and $N_2{}^+$ lines Measured spectrum presents several lines for diatomic molecule dinitrogen, including strongest lines. Is observed the Second Positive System for N_2 transition $C^3\Pi \rightarrow B^3\Pi$ and the First Negative System for $N_2{}^+$ transition $B^2\Sigma \rightarrow X^2\Sigma$, in table 1.3 peak values ([2], [3]). For N_2 is found also a band of multiple rotational lines centered around 336.58 ± 0.01 nm. Some of the peaks are seen in the second diffraction order, where there is more distance between lines. In figure 1.4 are presented two zooms for N_2 lines.

Atomic lines Are observed other lines from elements present in the plume ([10]):

- $\mathbf{H}_\alpha$ line corresponding to transition from quantum number $n = 3$ to $n = 2$

λ [nm]	I [arb.u.]
306.96 ± 0.01	53
307.11 ± 0.01	58
307.29 ± 0.01	62
307.94 ± 0.01	142
308.09 ± 0.01	148
308.26 ± 0.01	161
308.43 ± 0.01	112
308.62 ± 0.01	46
308.74 ± 0.01	137
309.11 ± 0.01	151
309.22 ± 0.01	120
309.45 ± 0.01	36
309.73 ± 0.01	125

Table 1.2: Peaks measured for OH.

	λ [nm]	I [arb.u.]	$(\nu' - \nu'')$
N_2	316.03 ± 0.01	381	(1-0)
	337.11 ± 0.01	1000	(0-0)
	357.77 ± 0.01	722	(0-1)
N_2	367.22 ± 0.20	58	(3-5)
	371.12 ± 0.04	172	(2-4)
	375.66 ± 0.02	232	(1-3)
	380.64 ± 0.02	423	(0-2)
N_2^+	391.50 ± 0.02	355	(0-0)
	427.45 ± 0.02	180	(0-1)

Table 1.3: Peaks measured for N_2 and N_2^+.

	λ [nm]	I [arb.u.]
H_α	655.96 ± 0.04	113
He	586.94 ± 0.05	122
	705.56 ± 0.01	649
O	776.89 ± 0.01	393

Table 1.4: Main peaks measured for other species found in plasma.

- **He** two of the strongest lines for helium
- **O** strong line of oxygen

1.4 Relative intensities

It's studied spectra variation changing experimental setup: pulse settings and measurements position. Intensities are evaluated for OH and N_2 species, collectively for the lines in a wavelength range specific for the peaks. For OH lines is considered all the rotational band between 306-309 nm, lines for N_2 are separated in those between 335-337 nm (rotational band and (0-0) transition) and those between 368-382 nm (vibrational transitions with $\Delta\nu = 2$).

Pulse frequency OH lines for both positions have same intensity with low and medium power setup, while is lower with higher frequency, with similar behavior in both positions. N_2 intensities also decrease with higher frequencies, for every lines, it reaches around 0.6% for $f = 15\,\text{kHz}$ in position 1, and lower values for position 2. It seems that production of those reactive species have rates dependant from pulse frequency, for high frequency there might be more relevant competitor reactions.

Sight position At 10 mm from the source, in position 2, intensities for OH decreases drastically, under 0.1% of values in position 1. OH species seems to have small lifetime or mobility, so deposition of this species is higher when closer to the target. For N_2 intensities are equal at low frequency for both positions, while for higher frequencies they decrease more for position 2. For low frequency, concentration of excited N_2 is high so even distant from the target we have high radiation emission. When it decreases, for higher frequencies, concentration lowers and we have few molecules that reach the target.

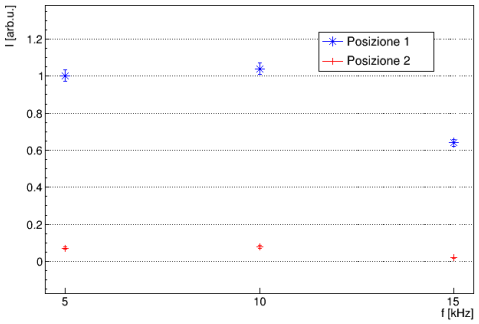

(a) OH intensities in range 306-309 nm

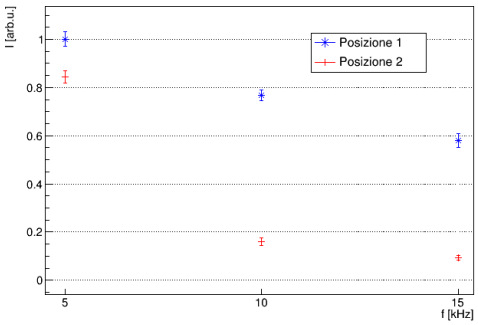

(b) N_2 intensities range 335-337 nm

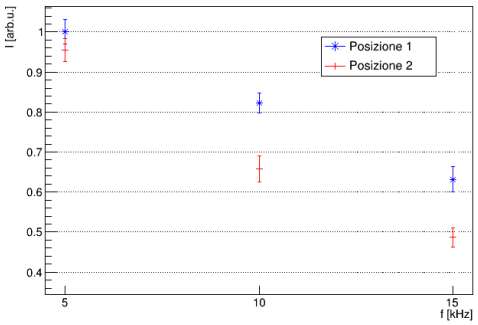

(c) N_2 intensities range 368-382 nm

Figure 1.5: Relative intensities in selected portions of the spectrum, for different frequencies, in blue for position 1 in red for position 2.

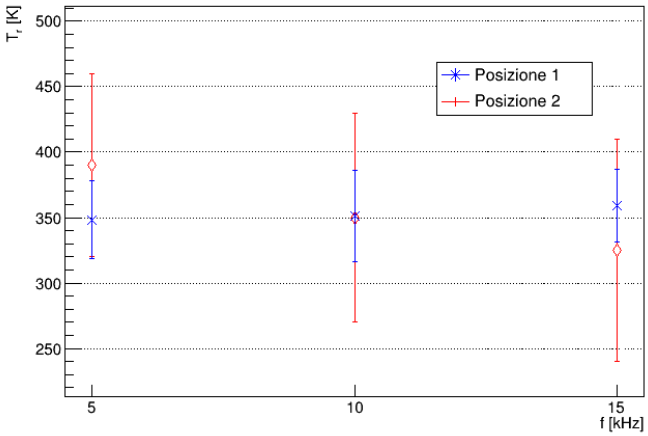

Figure 1.6: Estimation of rotational temperature of OH molecule, for different frequencies, in blue position 1 in red position 2.

1.5 Estimation of plasma temperatures

Possible to estimate plasma composition parameters. Rotational = temperature of ions, vibrational = storage energy.

1.5.1 Rotational temperature for OH

How, simulation, article.

1.5.2 Rotational temperature for N_2

How, simulation, article.

1.5.3 Vibrational temperature for N_2

How, boltzmann graph, article.

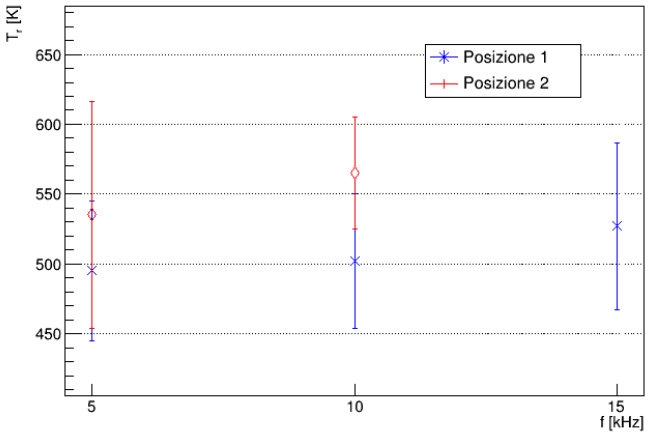

Figure 1.7: Estimation of rotational temperature of N_2 molecule, for different frequencies, in blue position 1 in red position 2.

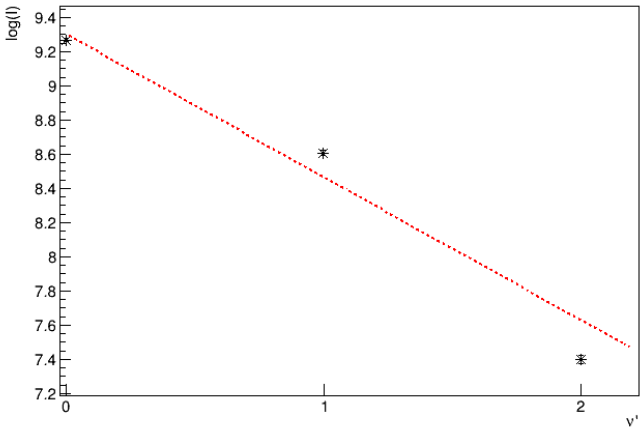

Figure 1.8: Example of a boltzmann graph for estimation of vibrational temperature, for low pulse setup and position 1.

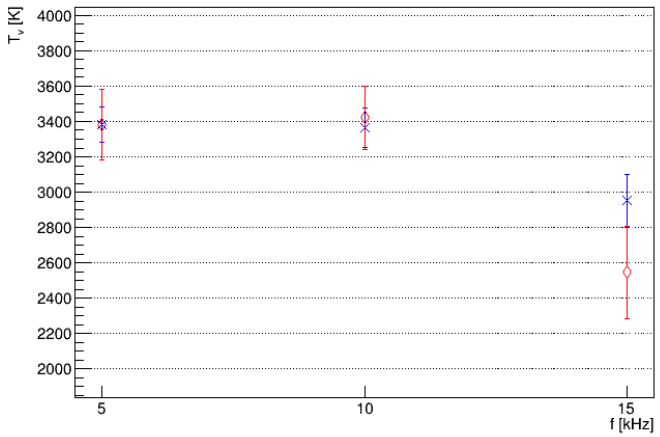

Figure 1.9: Estimation of vibrational temperature of OH molecule, for different frequencies, in blue position 1 in red position 2.

Bibliography

[1] Hans-Joachim Kunze (auth.) *Introduction to Plasma Spectroscopy*. 1st ed. Springer Series on Atomic, Optical, and Plasma Physics 56. Springer-Verlag Berlin Heidelberg, 2009. ISBN: 9783642022326,3642022324.

[2] S. B. Bayram and M. V. Freamat. "Vibrational spectra of N2: An advanced undergraduate laboratory in atomic and molecular spectroscopy". In: *American Journal of Physics* 80.8 (2012), pp. 664–669. DOI: 10.1119/1.4722793. eprint: https://doi.org/10.1119/1.4722793. URL: https://doi.org/10.1119/1.4722793.

[3] N Britun et al. "Determination of the vibrational, rotational and electron temperatures in N2and Ar–N2rf discharge". In: *Journal of Physics D: Applied Physics* 40.4 (2007), pp. 1022–1029. DOI: 10.1088/0022-3727/40/4/016. URL: https://doi.org/10.1088%2F0022-3727%2F40%2F4%2F016.

[4] Nisha Chandwani et al. "Determination of Rotational, Vibrational and Electron Temperatures in Dielectric Barrier Discharge in air at atmospheric pressure". In: (June 2014). DOI: 10.13140/RG.2.1.2078.6725.

[5] Ioana Gerber et al. "Air Dielectric Barrier Discharge Plasma Source For In Vitro Cancer Studies". In: *Clinical Plasma Medicine* 9 (Feb. 2018), p. 4. DOI: 10.1016/j.cpme.2017.12.006.

[6] Gerhard Herzberg. *Molecular Spectra and Molecular Structure I: Spectra of Diatomic Molecules*. 2nd. D. Van Nostrand, 1950. ISBN: 9780442033859,0442033850.

[7] C. de IZARRA. "COMPUTER SIMULATION OF THE UV OH BAND SPECTRUM". In: *International Journal of Modern Physics C* 11.05 (2000), pp. 987–998. DOI: 10.1142/S0129183100000857. eprint: https://doi.org/10.1142/S0129183100000857. URL: https://doi.org/10.1142/S0129183100000857.

[8] Andre Knie. "Photon induced inner-shell excitation processes of nitrous oxide probed by angle resolved fluorescence and Auger-Electron spectrometry". Dr. Kassel: Univ. Kassel, 2013. ISBN: 978-3862194582.

[9] I A Kossyi et al. "Kinetic scheme of the non-equilibrium discharge in nitrogen-oxygen mixtures". In: *Plasma Sources Science and Technology* 1.3 (1992), pp. 207–220. DOI: 10.1088/0963-0252/1/3/011. URL: https://doi.org/10.1088%2F0963-0252%2F1%2F3%2F011.

[10] A. Kramida et al. 2018.

[11] S. P. Kuo et al. "Applications of Air Plasma for Wound Bleeding Control and Healing". In: *IEEE Transactions on Plasma Science* 40.4 (2012), pp. 1117–1123. ISSN: 0093-3813. DOI: 10.1109/TPS.2012.2184142.

[12] H.A. Van Sprang, H.H. Brongersma, and F.J. De Heer. "Absolute emission cross sections for the calibration of optical detection systems in the 120–250 nm range". In: *Chemical Physics Letters* 65.1 (1979), pp. 55 –60. ISSN: 0009-2614. DOI: https://doi.org/10.1016/0009-2614(79)80124-4. URL: http://www.sciencedirect.com/science/article/pii/0009261479801244.

[13] Wikipedia contributors. *Vibronic spectroscopy*. 2018. URL: https://en.wikipedia.org/w/index.php?title=Vibronic_spectroscopy&oldid=823782704.